Title

Towards the identification of multi-parametric quantitative MRI biomarkers in lupus nephritis

Journal

Magnetic Resonance Imaging, 33(9)

ISSN

0730-725X

Authors

Rapacchi, Stanislas
Smith, Robert X
Wang, Yi
et al.

Publication Date

2015-11-01

DOI

10.1016/j.mri.2015.06.019

Peer reviewed

Magnetic Resonance Imaging xxx (2015) xxx–xxx

Contents lists available at ScienceDirect

Magnetic Resonance Imaging

journal homepage: www.mrijournal.com

Towards the identification of multi-parametric quantitative MRI biomarkers in lupus nephritis ☆

Stanislas Rapacchi [a], Robert X. Smith [b], Yi Wang [b], Lirong Yan [b], Victor Sigalov [a], Kate E. Krasileva [b], George Karpouzas [c], Adam Plotnik [a], James Sayre [a], Elizabeth Hernandez [c], Ajay Verma [d], Linda Burkly [d], Nicolas Wisniacki [d], Jaime Torrington [d], Xiang He [e], Peng Hu [a], Ping-Chun Chiao [d], Danny J.J. Wang [a,b,*]

[a] Department of Radiology, University of California Los Angeles, Los Angeles, CA, USA
[b] Department of Neurology, University of California Los Angeles, Los Angeles, CA, USA
[c] Department of Rheumatology, Harbor-UCLA Medical Center, Los Angeles, CA, USA
[d] Biogen Idec, Cambridge, MA, USA
[e] Department of Radiology, State University of New York at Stony Brook, Stony Brook, NY, USA

ARTICLE INFO

Article history:
Received 5 March 2015
Revised 16 June 2015
Accepted 21 June 2015
Available online xxxx

Keywords:
Renal function
Multi-parametric quantitative MRI (qMRI)
Arterial spin labeling (ASL)
Blood oxygen level dependent (BOLD)
T1rho MRI
Lupus nephritis (LN)

ABSTRACT

Purpose: To identify potential biomarkers of the renal impairment in lupus nephritis using a multi-parametric renal quantitative MRI (qMRI) protocol including diffusion weighted imaging (DWI), blood oxygen level dependent (BOLD), arterial spin labeling (ASL) and T1rho MRI between a cohort of healthy volunteers and lupus nephritis (LN) patients.
Materials and methods: The renal qMRI protocol was performed twice with repositioning in between on 10 LN patients and 10 matched controls at 1.5 T. Navigator-gated and breath-hold acquisitions followed by non-rigid image registration were used to control respiratory motion. The repeatability of the 4 MRI modalities was evaluated with the intra-class correlation coefficient (ICC) and within-subject coefficient of variation (wsCV). Unpaired t-test and stepwise logistic regression were carried out to evaluate qMRI parameters between the LN and control groups.
Results: The reproducibility of the 4 qMRI modalities ranged from moderate to good (ICC = 0.4–0.91, wsCV ≤ 12%) with a few exceptions. T1rho MRI and ASL renal blood flow (RBF) demonstrated significant differences between the LN and control groups. Stepwise logistic regression yielded only one significant parameter (medullar T1rho) in differentiating LN from control groups with 95% accuracy.
Conclusion: A reasonable degree of test–retest repeatability and accuracy of a multi-parametric renal qMRI protocol has been demonstrated in healthy volunteers and LN subjects. T1rho and ASL RBF are promising imaging biomarkers of LN.

1. Introduction

Lupus nephritis (LN) affects over half of all patients with systemic lupus erythematosus (SLE), even those without clinical manifestations of renal disease. This condition increases mortality and morbidity rates among patients due to, among other reasons, the risk of chronic kidney disease with the need for renal transplant in approximately 25% of cases. Lupus nephritis is mostly diagnosed in women in their thirties and is the primary cause of systemic disease with secondary renal involvement [1]. Available clinical endpoints in LN to assess response to treatment have limited utility, as they may not directly reflect renal histopathological features that have been associated with poor prognosis [2]. Histopathological renal inflammatory activity and/or damage may persist despite clinically silent disease after treatment. Furthermore, histological renal damage may take a long time to become clinically evident as assessed by currently available clinical biomarkers (e.g., doubling serum creatinine).

Recent Food and Drug Administration (FDA) guidance for the development of treatments for LN suggests that, when feasible, renal biopsies should be obtained at the end of a trial evaluating renal response or remission to demonstrate that an improved renal response corresponds to a histologic improvement, including effects on the percent of sclerosed glomeruli [3]. However, the adoption of repeat biopsy in a clinical trial setting has been and it is expected to continue to be very low. Renal imaging may provide important markers of kidney diseases through the evaluation of the morphology, function and metabolism of the kidney. During recent years, several magnetic resonance imaging (MRI) techniques have shown promises as imaging biomarkers for kidney diseases [4]. These MRI

☆ Grant support: This study was sponsored by Biogen Idec.
* Corresponding author at: Department of Neurology, University of California Los Angeles, 660 Charles E Young Dr South, Los Angeles, CA 90095, USA. Tel.: 310-983-3667, Fax: 310-794-7406.
E-mail address: jwang71@gmail.com (D.JJ. Wang).

http://dx.doi.org/10.1016/j.mri.2015.06.019
0730-725X/

techniques include diffusion weighted imaging (DWI), blood-oxygenation-level dependent (BOLD) imaging, perfusion imaging with arterial spin labeling (ASL), and T1rho MRI. DWI measures apparent diffusion coefficient (ADC) values and quantifies the combined effects of blood microcirculation and Brownian motion of water molecules within the interstitial space [5,6]. DWI studies on kidney diseases revealed that patients with renal failure have significantly lower ADC values in the cortex and medulla than normal healthy volunteers [7]. More recently, this technique was successfully used to demonstrate a correlation between ADC reductions and renal fibrosis in ligated kidneys in a mouse unilateral urethral obstruction model of interstitial fibrosis [8]. BOLD MRI noninvasively assesses tissue oxygen bioavailability by measuring relative changes in deoxyhemoglobin, an endogenous paramagnetic contrast agent. Quantitative BOLD MRI R2* values have been demonstrated experimentally to correlate to acute and transient changes in oxygenation levels in the renal cortex and medulla [9,10]. Additionally, the capability of BOLD MRI to evaluate chronic, progressive, parenchymal hypoxia in renal allografts has been reported [11].

Given that subjects with renal dysfunction are generally not suitable for contrast agents, ASL offers an appealing approach for renal perfusion imaging by utilizing magnetically labeled arterial blood water as an endogenous tracer. With recent technical developments to effectively control respiratory motion, ASL MRI approaches have been shown to provide reliable and quantitative kidney perfusion measurements in clinical settings [12,13]. T1rho MRI is another emerging MRI technique that is sensitive to the presence of macromolecules (such as collagen and proteoglycan [14]). A preclinical study in a rat biliary duct ligation (BDL) model demonstrated that T1rho imaging detected liver fibrosis in BDL rats and that the degree of fibrosis correlated with the degree of increase in T1rho measurements [15].

All four MRI techniques, as described above, are non-contrast and quantitative, and can be applied longitudinally to monitor disease progression and/or treatment effects. The combination of the four techniques is likely to provide a multi-modality evaluation of renal function, and may provide more accurate characterization or staging of kidney diseases such as LN than each individual technique alone. The primary aim of the present study was to develop a multi-parametric renal qMRI protocol and evaluate its test–retest repeatability in a cohort of LN patients and healthy normal volunteers (HN). The secondary aim was to evaluate the clinical utility of the multi-parametric renal quantitative MRI protocol in differentiating LN patients from HN subjects.

2. Material and methods

2.1. Subjects recruitment

This study received institutional review board approval and informed consent was obtained from all subjects. Ten healthy volunteers (age = 29.4 ± 5.0 years, 8 F) and 10 biopsy-confirmed LN patients (age = 31.8 ± 6.2 years, 8 F) were recruited in this study. All subjects underwent a screening visit within 7 days prior to MRI to determine their eligibility for the study. The general inclusion criteria were: 1) age 18–60 years and 2) ability to understand study procedures and provide informed consent. The general exclusion criteria were: 1) contraindication for MRI or claustrophobia and 2) positive pregnancy test. Normal healthy volunteers were deemed healthy by the Investigator, based on the following assessments at screening: physical examination, medical history, vital signs, and clinical laboratory measurements of blood and urine samples (Covance Inc., Princeton, NJ, USA). Healthy volunteers with the following conditions were excluded: 1) receiving treatment with any prescription medication within 2 weeks before screening with the exception of contraceptives for women of childbearing potential, and 2) clinically significant abnormal clinical laboratory test values at Screening. LN patients had a documented diagnosis of SLE according to current American College of Rheumatology (ACR) criteria and a documented renal biopsy with diagnosis of LN. Exclusion criteria for the LN group included: 1) history of renal transplant and 2) subjects with uncontrolled diabetes or other condition that may result in significant renal disease.

2.2. MRI scanning and protocol

MRI experiments were performed on a 1.5 Tesla Siemens Avanto MR scanner (Erlangen, Germany), using an 8-channel flexible body array and the spinal array coil as the receiver. Each subject underwent two consecutive MRI sessions, with complete repositioning in between, in order to assess the reproducibility of the renal multi-parametric qMRI protocol. Each MRI session began with conventional 3D T1 weighted (T1w) volumetric interpolated breath-hold (VIBE, TR/TE = 4.5/1.6 ms, resolution = $1.1 \times 1.1 \times 2.5$ mm^3) and 2D multi-slice coronal and axial T2 weighted (T2w) HASTE (Half Fourier Acquisition Single Shot Turbo Spin Echo) scans (TR/TE = 800/54 ms, resolution = $1.3 \times 1.3 \times 6$ mm^3) that were used as anatomical localizers for both the kidneys and renal arteries. The renal qMRI protocol consisted of 4 quantitative MRI sequences including DWI, BOLD, T1rho and pseudo-continuous ASL (pCASL). In addition, phase-contrast (PC) MRI was performed to estimate the global renal blood flow (RBF) for comparison with renal perfusion measurements using pCASL. The duration of each MRI session ranged from 30 to 45 min, and the total duration of 2 repeated MRI sessions was less than 1.5 hr.

Table 1 lists the imaging parameters of the 4 sequences for the renal quantitative MRI protocol along with PC MRI. In order to balance the burden of breath holding and fast scans, two strategies were applied for controlling respiratory motion: 1) breath-holds (BH) that lasted no longer than 18 s each and performed at the end of expiration for BOLD, T1rho and PC MRI scans; and 2) navigator gated free-breathing (NavFB) acquisitions that were matched to be acquired during the end-expiration phase for DWI and pCASL scans. The navigator used a pencil-beam spin echo placed on the right diaphragm at the liver–lung interface with a ±5 mm acceptance range. DWI was performed using the product DW single-shot spin-echo EPI sequence with 7 *b*-values ranging from 0 to 700 s/mm^2. Based on our pilot study and literature [16], the DWI scan was repeated twice which were averaged to improve the reliability of exponential fitting. BOLD MRI was acquired using the product multi-echo gradient echo (GRE) sequence in 3 concatenated breath-holds, with 12 incremental TEs between 2.2 and 43.7 ms that were in-phase for water and fat signals. For both DWI and BOLD MRI, 10 coronal slices were acquired for a complete coverage of the kidneys.

Both T1rho [14] and pCASL [17] MRI used custom sequences developed in-house. A single oblique-coronal slice through both kidneys was imaged using a single-shot balanced steady-state free precession (bSSFP) sequence. The imaging slice was prescribed to be parallel to the descending aorta to avoid artifacts related to pulsatile aortic flow. A pre-saturation pulse was applied on the imaging slice at the beginning of each TR for both T1rho and pCASL scans. During T1rho preparation, the previously reported approach using a continuous train of spin-locking hard pulses interleaved with adiabatic refocusing pulses ($N = 4$) [14,18] was used to minimize artifacts associated with B0 (background magnetic field) and B1 (RF transmission) imperfection. Spin-locking hard pulses used a B1 magnitude of 10 μT, which is positioned at a smooth and stable portion of the renal tissue T1rho dispersion curve. A total of 4 repetitions with incremental spin lock times (TSL = 10, 30, 50, 70 ms) enabled T1rho quantification. The axial pCASL labeling plane was placed approximately 10 cm above the center of kidneys

Please cite this article as: Rapacchi S, et al, Towards the identification of multi-parametric quantitative MRI biomarkers in lupus nephritis, Magn Reson Imaging (2015), http://dx.doi.org/10.1016/j.mri.2015.06.019

Table 1
Imaging parameters for the 5 MRI sequences of the renal qMRI protocol.

Imaging Sequence	BOLD	DWI	T1rho	pCASL	PC-MRI
Matrix	192 × 192 × 10	128 × 128 × 10	128 × 128	128 × 128	320 × 320
Resolution (mm^3)	1.9 × 1.9 × 5 (10 slices)	2.7 × 2.7 × 5 (10 slices)	2.7 × 2.7 × 5 (1 slice)	2.7 × 2.7 × 5 (1 slice)	0.9 × 0.9 × 7 (1 slice)
Respiratory control	3BH	NavFB	1BH	NavFB	1BH
Readout sequence	Multi-echo GRE	Spin-echo EPI	bSSFP	bSSFP	GRE
TE/TR (ms)	(2.2–43.7)/187	65/1100	1.9/2000	1.9/3700	2.89/4.7
Imaging time	3 × 17 s	3–5 min	17 s	3–5 min	20 s
FA (°)	25	90	70	70	30
BW (Hz/Px)	330	2170	558	558	504
Specific parameters	12 echoes in-phase for water and fat	b = 0, 50, 100, 150, 200, 250, 300, 400, 500, 600, 700 s/mm^2, 2 averages, 3 encoding directions: x–y–z	B1 = 10uT, TSL = 10, 30, 50, 70 ms	Label duration = 2 s, PLD = 1.2 s, 30 acquisitions	Tres = 60 ms

*BH: breath-hold; NavFB: navigator-gated free breathing; EPI: echo-planar imaging; GRE: gradient-echo; bSSFP: balanced steady state free precession; PLD: post-labeling delay; TSL: time of spin-lock; Tres: temporal resolution.

(Fig. 1). Detailed parameters for T1rho and pCASL sequences can be found in Refs. [14,17,19]. PC-MRI was performed in an oblique-sagittal plane placed perpendicular to the renal artery of each kidney respectively, based on T1w and T2w images. A pulse-oxymetry was used to synchronize the subject's cardiac cycle, resulting in a temporal resolution of 60 ms for PC MRI scans.

2.3. Image post-processing

Raw DICOM images of the 4 sequences were transferred and processed off-line using custom pipelines including ANTs (Advanced Normalization Tools, http://picsl.upenn.edu/software/ants/), OsiriX (Osirix foundation, Geneva, Switzerland) and Matlab (Mathworks, Natick, MA). To minimize residual motion (particularly in navigator-gated scans), a non-rigid body motion correction was applied by maximizing the cross-correlation between image frames using symmetric diffeomorphic image registration by the ANTs software [20,21]. Afterwards, all images were brought in Osirix for image quality assessment, parameter quantification and region-of-interest (ROI) analyses. Quantitative T2* values were fitted from the BOLD scan using the OsiriX T2 Fit Map plugin. For DWI, ADC values were fitted using the OsiriX ADCmap plugin to generate ADC maps, using b values $\geq$200 s/mm^2 to minimize the effect of microvascular flow on tissue ADC values [22,5,6].

RBF was calculated using custom program in Matlab (Mathworks, Natick, MA) in units of mL/100 g/min using the pCASL scan [23]:

$$\mathrm{RBF} = \frac{\lambda \Delta M}{2\alpha T_{1b} M_C} \frac{1}{exp(-w/T_{1b}) - exp(-(\tau + w)/T_{1b})} \quad (1)$$

where ΔM is the mean difference signal, M_C is the mean control magnetization, α is the labeling efficiency (0.74 based on a flow phantom study), λ is the blood/tissue water partition coefficient (0.9 g/mL), T_{1b} (1.3 s at 1.5 T) is the longitudinal relaxation time of water in the blood, τ (2 s) is the labeling duration, and w (1.2 s) is the post-labeling delay. Eq. (1) assumes that the labeled blood stays in the vasculature rather than completely exchanging into the tissue compartment, which may lead to underestimation of perfusion, since kidney tissue T1 (~1 s) is shorter than blood T1 (1.3 s). Nevertheless, our simulation indicated that this perfusion underestimation is only 5% based on the employed imaging parameters and an assumed arterial transit time of 1 s for the kidneys [24].

For T1rho, a mono-exponential decay model was fitted pixel-wise using a Levenberg–Marquardt algorithm in OsiriX, on the dataset of 4 TSLs ranging from 10 to 70 ms with a step of 20 ms, using the equation:

$$S(\mathrm{TSL}) = S_0 e^{-\frac{\mathrm{TSL}}{T1\rho}} \quad (2)$$

To account for signal recovery during the readout echo train, a fully saturated image acquired within the same breath-hold, was subtracted from all T1rho-weighted images before curve fitting.

PC-MRI analysis was performed online after the MRI exam using the manufacturer software package (Argus, Siemens, Germany). A region-of-interest (ROI) was manually drawn on the cross-section of the renal artery on one time frame image, which was then propagated in time and adjusted using the complex difference images. Mean flow velocity was extracted using the phase values in the ROI across the cardiac cycle. The product of the mean flow velocity and cross-sectional area of the renal artery provided estimate of mean global RBF.

2.4. Statistical analysis

Regions-of-interest (ROIs) of cortex and medulla were manually drawn by trained researchers on each scan of the 4 MRI modalities on the left and right kidney respectively, using corresponding T1w and T2w MRI (similar slice position) as references (Fig. 2a). The cortical ROI (C-shape) was drawn along the edge of kidneys and the medullar ROI was defined as wedge shaped islands (N = 2-3) based on low intensity in T1w images and high intensity in T2w images. Care was taken to avoid the high intensity of the pelvis as well as occasional imaging artifacts such as signal dropouts due to B0 inhomogeneity and bSSFP banding artifacts. For BOLD and DWI, ROIs were drawn on the 2 center slices. The mean values of ADC, T2*, T1rho and RBF were extracted from the ROIs and were imported into SPSS (IBM Corp., Armonk, NY, USA) for statistical analysis. The reproducibility of MRI measurements was assessed across the 2 repeated scans using intraclass correlation coefficient (ICC) and within-subject coefficient of variation (wsCV). Bland–Altman (BA) [13] plots were used to show parameter dispersion and the bias and the confidence intervals between the 2 scans for each quantitative MRI parameter. In addition, image quality for each scan of the 4 modalities was evaluated using a 1–4 scale (1 being non-diagnostic, 2 being acceptable, 3 being good, and 4 being excellent).

The 2 repeated scans of each MRI modality were then averaged, as well as values from left and right kidneys. Statistical differences between healthy subjects and LN patients were assessed using unpaired t-test and stepwise binary logistic regression was performed to evaluate the capacity of renal quantitative MRI parameters for the classification of LN and HN groups.

3. Results

3.1. Subjects

Table 2 lists the demographic information and clinical characteristics of the 10 LN patients. The age range and 4:1 female to male ratio

Please cite this article as: Rapacchi S, et al, Towards the identification of multi-parametric quantitative MRI biomarkers in lupus nephritis, Magn Reson Imaging (2015), http://dx.doi.org/10.1016/j.mri.2015.06.019

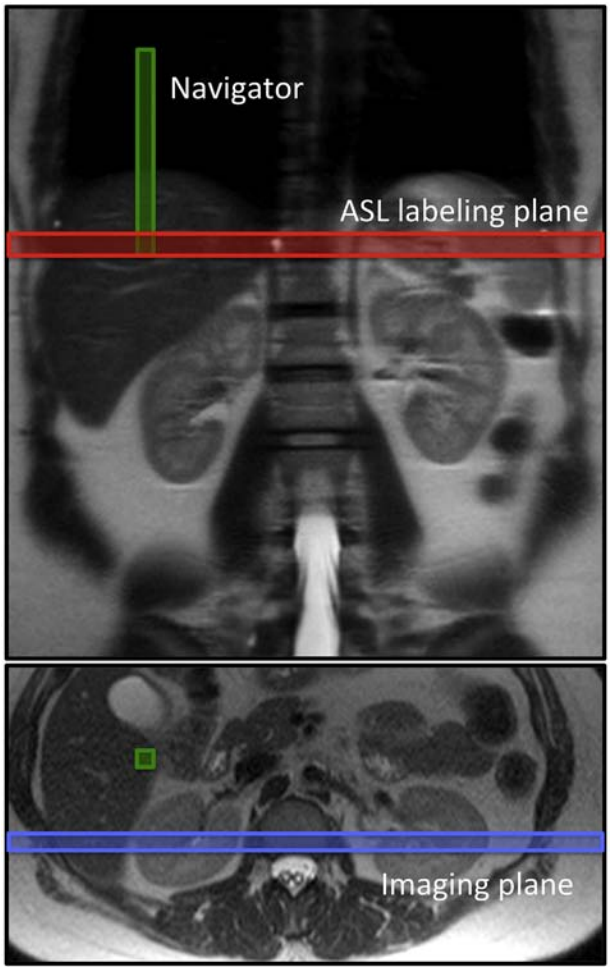

Fig. 1. Schematic positioning in coronal and axial views of the ASL labeling plane (1 line, red), navigator (axial plane, green) and imaging plane (coronal plane, blue) of renal pCASL. Other qMRI sequences followed the same coronal orientation depicted in blue.

were based on the prevalence of LN in women in their thirties. All LN patients underwent renal biopsy within 1 year before MRI with International Society of Nephrology/Renal Pathology Society (ISN/RPS) class 3 to 5 LN (focal, diffuse and membranous fibrosis respectively). All LN and HN subjects had normal estimated glomerular filtration rate (eGFR > 60 mL/min). There was no statistically significant differences of eGFR, age or gender between the LN and HN groups.

3.2. Image quality assessment

All scans were completed except that PC-MRI acquisition failed 4 times (out of 80) due to gradient interactions with the pulse-oxymetry trigger. Additionally one T1rho and 2 BOLD scans could not be interpreted due to image artifacts. Average image quality was rated good to excellent for all 4 sequences (2.5–3.4, Table 3). Figs. 2 and 3 show quantitative ADC, T2*, T1rho and RBF maps of a representative healthy subject and an LN subject respectively, demonstrating excellent image quality for all 4 modalities and negligible registration errors after post-processing with non-rigid motion correction using ANTs.

3.3. Test–retest repeatability

All test–retest results are reported in Fig. 4, separating HN and LN first, and then combining the 2 groups, and finally combining left and right kidneys. For healthy volunteers, all 4 quantitative MRI modalities showed moderate to good (ICC = 0.44–0.88) reproducibility in both the cortex and medulla (Fig. 4a), except for DWI in the left medulla (ICC = 0.15). The reproducibility was reduced and showed larger variability in LN patients (ICC range 0.12–0.94) with 6 out of 16 measurements below ICC of 0.4: ASL RBF in medulla, T1rho in left cortex, DWI in left cortex and medulla (highlighted in Fig. 3a). However, ICC for BOLD was increased in LN patients (0.8–0.94) compared to healthy subjects (0.6–0.88). When both HN and LN groups were combined, ICC results were more stabilized (0.17–0.91) with only 2 measurements below ICC of 0.4: T1rho in left cortex (0.38) and DWI in left medulla (0.17). When left and right kidney measurements were further combined (averaged), all 4 quantitative MRI modalities showed moderate to good reproducibility (ICC range 0.42–0.86) except DWI in medulla (ICC = 0.25).

The wsCV were generally below 13% for all 4 modalities across both LN and HN groups (Fig. 4b), except for ASL RBF in medulla

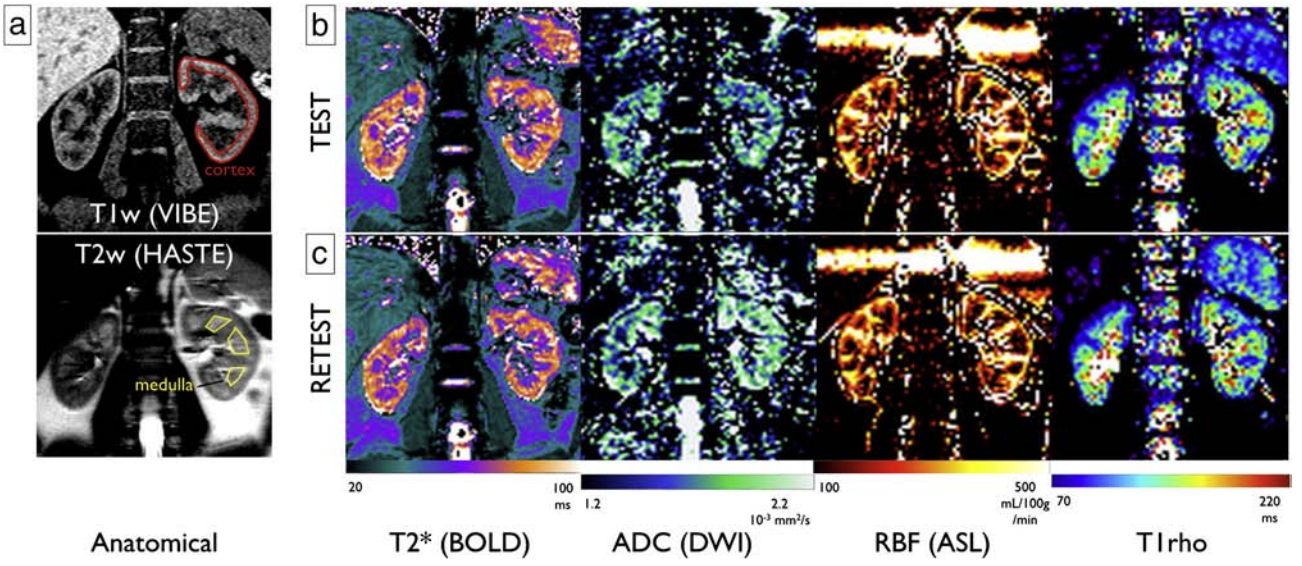

Fig. 2. Renal anatomical MRI scans (a), and 4 quantitative MRI modalities with repeated scans (b and c) in a healthy volunteer. Each parameter was quantified on both kidneys using regions-of-interest (ROIs) for both the cortex (red) and the medulla (yellow).

Please cite this article as: Rapacchi S, et al, Towards the identification of multi-parametric quantitative MRI biomarkers in lupus nephritis, Magn Reson Imaging (2015), http://dx.doi.org/10.1016/j.mri.2015.06.019

Table 2
Demographic and clinical characteristics of the healthy normal volunteers (HN) and lupus nephritis (LN) patients.

Subject ID	Age (y)	Gender	eGFR (mL/min)	Class ISN/RPS	Time since LN diagnostic (months)
HN	25	F	76		
	31	M	98		
	26	F	87		
	22	F	90		
	33	F	83		
	28	F	75		
	38	F	94		
	36	F	81		
	27	M	80		
	28	F	119		
	29.4 ± 5.0	8 F/2 M	88.3 ± 13.1		
LN	43	F	65	IV	7
	30	M	103	III	6
	28	F	66	III	6
	36	F	89	IV	51
	31	F	82	V	107
	26	F	187	III	62
	25	M	140	V	63
	36	F	128	IV	72
	38	F	78	V	8
	25	F	109	IV	63
	31.8 ± 6.2	8 F/2 M	104.7 ± 38.3	3 III/4 IV/3 V	

International Society of Nephrology/Renal Pathology Society (ISN/RPS) class was determined through renal biopsy within 1 year prior to MRI.

(wsCV = 18.6–22.7%). Fig. 5 shows the Bland–Altman plots of the 4 quantitative MRI modalities. Estimated BOLD T2* values showed excellent reproducibility (ICC > 0.8, wsCV < 6% for combined LN and HN groups) and clear contrast between the cortex (T2* = 83 ± 8 ms) and medulla (T2* = 60 ± 8 ms). ASL RBF measurements also provided excellent contrast between the cortex (RBF = 325 ± 63 mL/100 g/min) and medulla (RBF = 111 ± 31 mL/100 g/min) with good reproducibility in the cortex (ICC ≥ 0.6, wsCV = 10.9%-11.6%). Medullar RBF showed reduced reproducibility (ICC = 0.46–0.47, wsCV = 20.8–21.1%) probably due to low RBF and signal-to-noise ratio (SNR).

In addition, we found a significant correlation between global mean RBF from PC-MRI and cortical RBF from pCASL ($R = 0.53$, $p = 0.01$). PC-MRI was more reproducible in the left renal artery than in the right artery (ICC = 0.86/0.51, wsCV = 21.6%/28.7% for left/right kidney respectively). T1rho provided excellent contrast between the cortex (T1rho = 125 ± 17 ms) and medulla (T1rho = 175 ± 43 ms) with moderate test–retest repeatability (ICC ranging 0.38–0.76, wsCV = 5.9–9.6%). DWI showed poor contrast between the cortex (ADC = 1837 ± 99 × 10^{-6} mm^2/s) and medulla (ADC = 1795 ± 143 × 10^{-6} mm^2/s) with moderate to good reproducibility (ICC = 0.4–0.7, wsCV < 5%) except for left medulla (ICC = 0.17, wsCV = 9.5%).

3.4. Comparison between HN and LN groups

Table 3 lists the mean value and standard deviation (SD) of the 4 qMRI modalities measured in the left and right medulla and cortex of the HN and LN groups respectively. T1rho values measured in the medulla and cortex (both left and right side) were significantly increased in LN patients than in healthy volunteers (205 ± 50 ms vs. 145 ± 15 ms, $p < 0.001$ in the medulla, 136 ± 20 ms vs. 115 ± 8 ms, $p = 0.003$ in the cortex). ASL RBF was significantly increased in the right cortex (358 ± 63 mL/min/100 g vs. 295 ± 49 mL/min/100 g, $p = 0.046$) and in the right medulla (136 ± 32 mL/min/100 g vs. 96 ± 29 mL/min/100 g, $p = 0.015$). ASL RBF was also increased in the left cortex and medulla but did not reach statistical significance. BOLD and DWI did not show significant differences between LN and HN subjects. The stepwise logistic regression yielded only 1 parameter: medullar T1rho (T1rhom) in the model ($\chi^2 = 18.398$, $p < 0.001$). Using T1rhom, a success rate of 95% for the classification of LN and HN groups was achieved (1 LN patient was mislabeled out of 20 subjects). A receiver operating characteristic (ROC) analysis (Fig. 6) yielded a 94% [95% CI: 82%–100%] area under the curve ($p = 0.001$).

4. Discussion

The purpose of the present study was to evaluate the test–retest repeatability of a multi-parametric renal quantitative MRI protocol along with its clinical utility in a cohort of healthy volunteers and LN patients.

Table 3
Average values for test and retest experiment, within-subject coefficient of variation (wsCV), intraclass correlation coefficient (ICC) and average image quality for the 4 MRI modalities.

	HN test and retest	LN test and retest	*p*-Value	wsCV (%)	ICC	Quality
ASL RBF (ml/100 g/min)						
Left cortex	315 ± 44	341 ± 75	0.442	11.6	0.62	3.1 ± 0.8
Right cortex	295 ± 49	358 ± 63	**0.046**	10.9	0.66	
Left medulla	100 ± 27	116 ± 34	0.345	21.1	0.47	
Right medulla	96 ± 29	136 ± 32	**0.015**	20.8	0.46	
BOLD T2* (ms)						
Left cortex	82 ± 3	83 ± 11	0.983	2.2	0.91	3.4 ± 0.9
Right cortex	83 ± 3	82 ± 13	0.743	3.4	0.86	
Left medulla	57 ± 5	62 ± 11	0.224	5.1	0.84	
Right medulla	58 ± 5	61 ± 11	0.573	5.3	0.82	
T1rho (ms)						
Left cortex	120 ± 5	138 ± 19	**0.006**	5.9	0.38	3.0 ± 0.8
Right cortex	110 ± 6	133 ± 27	**0.013**	8.4	0.40	
Left medulla	152 ± 13	210 ± 47	**0.001**	9.6	0.51	
Right medulla	138 ± 10	199 ± 53	**0.005**	7.2	0.76	
DWI ADC (10^{-6} mm^2/s)						
Left cortex	1848 ± 88	1870 ± 187	0.688	2.7	0.61	2.5 ± 0.4
Right cortex	1821 ± 103	1809 ± 98	0.819	3.1	0.70	
Left medulla	1823 ± 198	1740 ± 213	0.327	9.5	0.17	
Right medulla	1844 ± 115	1771 ± 156	0.245	4.9	0.40	

Bold values indicate significance at p < 0.05.

Please cite this article as: Rapacchi S, et al, Towards the identification of multi-parametric quantitative MRI biomarkers in lupus nephritis, Magn Reson Imaging (2015), http://dx.doi.org/10.1016/j.mri.2015.06.019

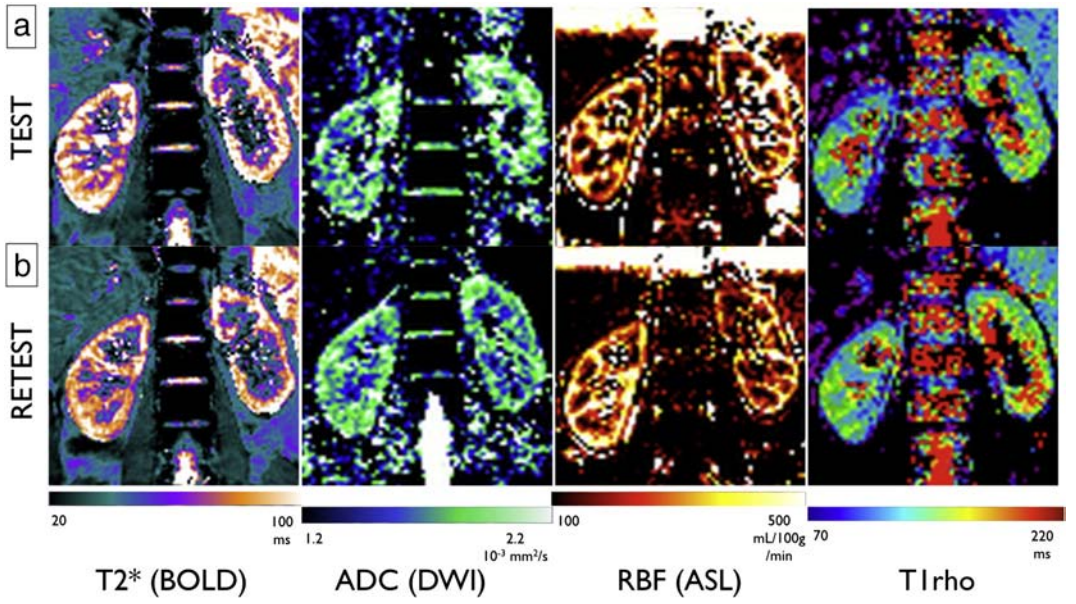

Fig. 3. Renal MRI scans of the 4 quantitative MRI modalities with repeated scans (a and b) in a lupus nephritis patient.

a

ICC	HN	LN	Combine HN&LN	Combine L&R
ASL LC	0.53	0.68	0.62	0.72
ASL RC	0.61	0.72	0.66	
ASL LM	0.53	0.39	0.47	0.46
ASL RM	0.66	0.12	0.46	
BOLD LC	0.61	0.94	0.91	0.86
BOLD RC	0.63	0.89	0.86	
BOLD LM	0.60	0.91	0.84	0.80
BOLD RM	0.88	0.80	0.82	
T1rho LC	0.46	0.38	0.38	0.42
T1rho RC	0.44	0.41	0.40	
T1rho LM	0.47	0.52	0.51	0.60
T1rho RM	0.51	0.78	0.76	
DWI LC	0.77	0.24	0.61	0.63
DWI RC	0.74	0.61	0.70	
DWI LM	0.15	0.26	0.17	0.25
DWI RM	0.44	0.37	0.40	

1

0

b

wsCV	HN	LN	Combine HN&LN	Combine L&R
ASL LC	12.4	10.7	11.6	11.3
ASL RC	12.8	8.9	10.9	
ASL LM	20.9	21.4	21.1	20.9
ASL RM	22.7	18.6	20.8	
BOLD LC	2.2	2.1	2.2	2.8
BOLD RC	2.8	4.0	3.4	
BOLD LM	5.8	4.4	5.1	5.2
BOLD RM	3.0	7.7	5.3	
T1rho LC	3.7	7.9	5.9	7.2
T1rho RC	5.2	11.3	8.4	
T1rho LM	6.4	12.4	9.6	8.4
T1rho RM	5.0	9.2	7.2	
DWI LC	2.2	3.2	2.7	2.9
DWI RC	3.5	2.6	3.1	
DWI LM	12.7	6.4	9.5	7.2
DWI RM	5.3	4.5	4.9	

25 %

0

Fig. 4. Test–retest repeatability results measured by ICC (a) and wsCV % (b) in left and right cortex (LC and RC), left and right medullar (LM and RM) in the healthy volunteers (HN) and lupus nephritis patients (LN) groups respectively.

Please cite this article as: Rapacchi S, et al, Towards the identification of multi-parametric quantitative MRI biomarkers in lupus nephritis, Magn Reson Imaging (2015), http://dx.doi.org/10.1016/j.mri.2015.06.019

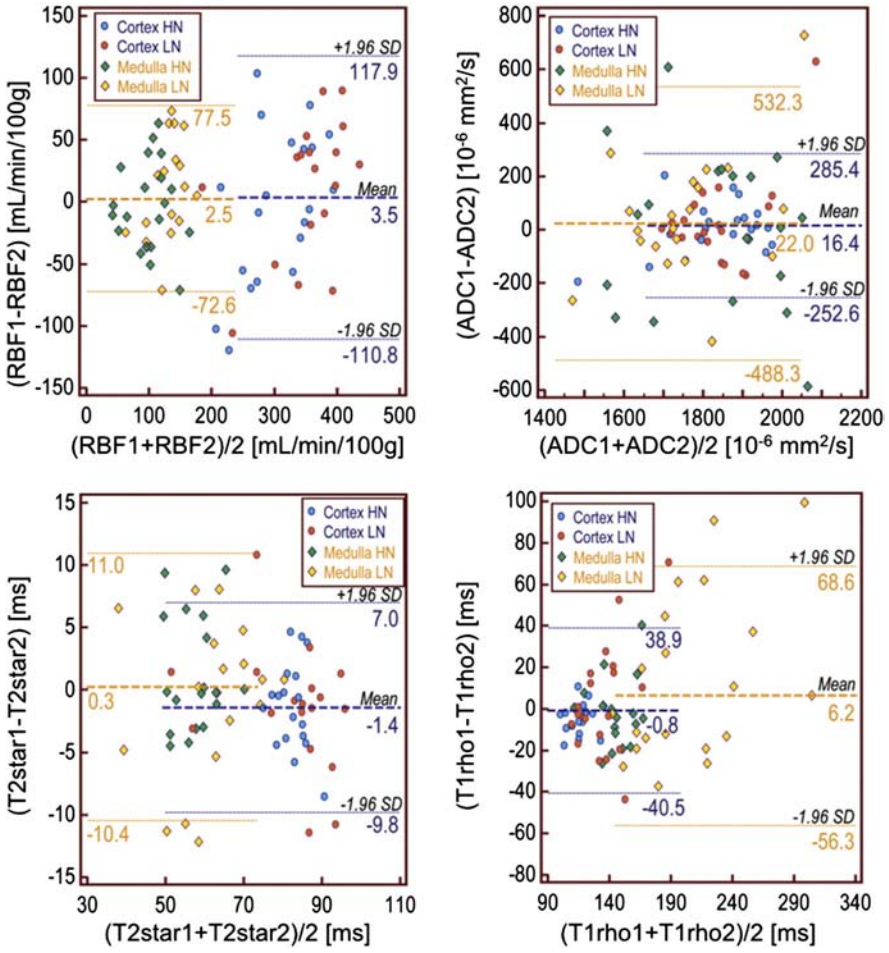

Fig. 5. Bland–Altman plots for the 4 quantitative MR parameters in the cortex and medulla. Lupus nephritis (LN) patients are separated from healthy normal (HN) volunteers. Units are in ml/min/100 g for ASL RBF, in 10–6 mm^2/s for DWI ADC, in ms for BOLD T2* and in ms for T1rho.

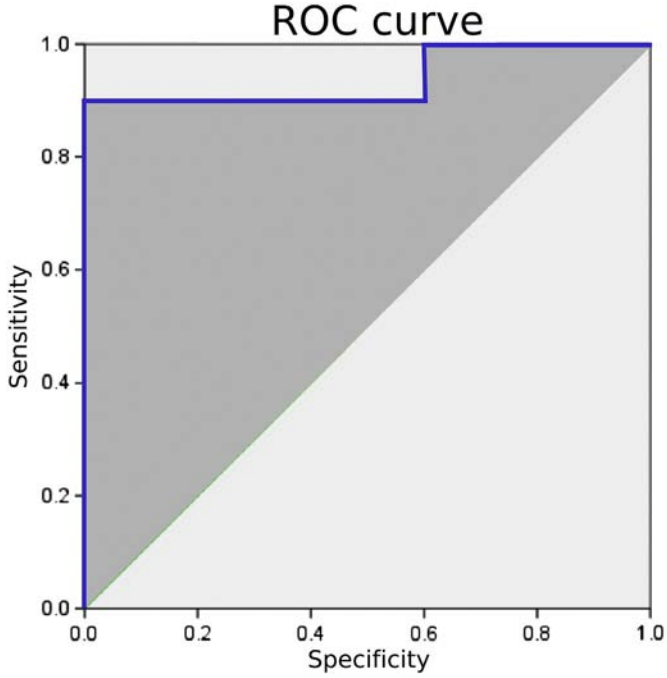

Fig. 6. ROC analysis from a regression model including only T1rho measures in the medulla (T1rhom). Area under the curve is 94% [95% confidence interval: 82–100%].

Please cite this article as: Rapacchi S, et al, Towards the identification of multi-parametric quantitative MRI biomarkers in lupus nephritis, Magn Reson Imaging (2015), http://dx.doi.org/10.1016/j.mri.2015.06.019

In the whole group of 10 healthy volunteers and 10 LN patients, the reproducibility of the 4 MRI modalities ranged from moderate to good (ICC = 0.4–0.91, wsCV ≤ 12%) with two exceptions (left medullar DWI and left cortical T1rho). As expected, the 4 quantitative MRI techniques were more reliable in healthy volunteers than in LN patients likely due to their variable physical conditions and potentially limited capability for motion control (e.g., breath-holding). The observed repeatability of the 4 qMRI techniques was comparable or slightly better than those reported in literature. For example, the reproducibility of R2* (1/T2*) measurement has been reported to be 3–12% by multiple studies [11,25,26]. A recent study reported a wsCV of 18% and 25% for ASL and dynamic contrast-enhanced (DCE) RBF measurement respectively [27]. The estimated MRI parameters (ADC, T2*, RBF and T1rho) in healthy volunteers also match well with reported values in literature for each modality respectively (RBF: [27], T2*: [26], ADC: [22] and T1rho: [14]). In addition, pCASL RBF measurement was validated using global RBF by PC MRI. Overall, our data suggest a reasonable degree of test–retest repeatability and accuracy for the proposed multi-parametric renal qMRI protocol. The employed strategies to control respiratory motion including navigator-gated and breath-hold acquisitions in conjunction with non-rigid motion correction using ANTs were generally successful, resulting in no obvious motion related artifacts in calculated quantitative maps. It is worth noting that ideally test–retest evaluation should be conducted on separate MRI scans on different days. Due to logistic constraints, we performed consecutive scans with patient repositioning in between to assess the repeatability of the qMRI protocol, assuming no changes in subjects' physiological condition.

During recent years, noninvasive assessment of renal function using MRI has gained considerable attention [28]. Renal function is characterized by different physiologic aspects, including perfusion, glomerular filtration, interstitial diffusion, tissue oxygenation and fibrosis, which can be assessed using ASL, DCE, DWI, BOLD and T1rho MRI respectively. The present study evaluated 4 non-contrast MRI modalities, and the results showed that T1rho is significantly prolonged in LN patients compared to healthy volunteers, and T1rho in medulla alone yields 95% accuracy for the differentiation between LN and HN groups in the cohort of 20 subjects. The biophysical mechanism underlying T1rho MRI is thought to be related to the proton exchange and dipole–dipole interactions between the free water pool and macromolecules (such as collagen and proteoglycan [29]). Increased T1rho has been reported in animal models of liver fibrosis with the degree of fibrosis correlated with the degree of increase in T1rho measurements [15]. Chronic kidney disease (CKD) due to LN is characterized by the progressive loss of kidney function resulting from chronic tubulointerstitial injury, which encompasses tubular atrophy and interstitial fibrosis. These renal damages, as well as persistent inflammatory activity, are regarded as major factors leading to the progression of CKD in LN. Increased T1rho in LN patients observed in the present study is consistent with their pathological results showing a variable degree of renal fibrosis (ISN/RPS class 3 to 5). Our data suggest that T1rho is a promising MRI modality for assessing renal function in LN and other kidney diseases, which awaits further clinical evaluation.

ASL RBF was also increased in LN patients compared to healthy volunteers, although statistical significance was only reached for the right kidney. The mechanism for increased RBF in LN patients is not well understood and may reflect inflammatory processes. ASL RBF measurement is emerging as a valuable MRI technique to assess renal function, and has been proposed as an imaging biomarker for renal cell carcinoma [30]. ASL MR studies have estimated renal perfusion at ~300 ml/100 g/min for the cortex and ~100 ml/100 g/min for the medulla of healthy kidneys [28]. Our data are highly consistent with previous studies, and add support to the validity of using ASL RBF for the characterization of renal function.

Past renal MRI studies have mainly focused on DWI and BOLD which are more clinically available. Significant correlations between ADC, BOLD R2* and GFR measurements as well as pathological findings have been reported in clinical populations with renal diseases [7,31,32]. However, controversial findings also exist. In an MRI study on 400 patients with chronic renal diseases at 1.5 and 3 T, no significant differences in R2* of the cortex and medulla were found between patient gender, age, eGFR, or between different stages of chronic kidney disease [33]. As BOLD is sensitive to changes in renal blood flow, blood volume and oxygen metabolism, there may not be a straightforward relationship between BOLD R2* (T2*) measurements and oxygen concentration (hypoxia) or disease stages in renal tissue. DWI is sensitive to the combined effects of microvascular flow and Brownian motion of water molecules within the interstitial space [5,6]. The estimated ADC values may be variable depending on the model (mono- or bi-exponential) and b values selected for fitting. In the present study, we used b values ≥ 200 s/mm^2 to minimize the effect of microvascular flow on tissue ADC values [22]. The resultant ADC values ($1.8 \pm 0.2 \times 10^{-3}$ mm^2/s in the cortex of healthy volunteers) are consistent with literature values of renal tissue ADC [22]. We also conducted bi-exponential fitting based on the IVIM model. However, the resultant perfusion fraction (f%) and pseudo-diffusion (D*) were not stable on a pixel-by-pixel basis. Bi-exponential model fitting was only stable when a fixed pseudo-diffusion (D*) value was assumed which may not be plausible for both the cortex and medulla. Our experience suggests that reliable IVIM analysis of renal DWI requires further technical optimization and clinical evaluation.

The choices of the 4 quantitative MRI techniques in the present study were made based on literature evidence of their (potential) sensitivity to renal function as well as scan durations within a clinically manageable time limit. We set the maximum allowed time for each technique to be 3–4 minutes, free breathing or with multiple breath holds. The total duration for the multi-parametric renal qMRI protocol including structural MRI scans was 30–40 min. There are alternative MRI techniques which were not included in our protocol, such as chemical-shift imaging [34] that are not directly related to renal function and MR spectroscopy [35], for which the duration of acquisition may be prohibitive. There are several limitations of the present study: 1) both ASL and T1rho MRI were single-slice. Recent renal ASL studies have used background suppressed 3D acquisitions to achieve full-kidney coverage, which can be adapted for our techniques [13,27]. 2) The sample size of 10 LN and 10 HN subjects was relatively small, especially for assessing test–retest repeatability in each group Therefore, our repeatability analysis was mainly based on the combined LN and HN groups. 3) LN patients were all under personalized medication for their condition, with a large panel of medications and medical history. 4) Our study focuses on lupus nephritis and its characterization through parametric MRI. ASL and T1rho remain MRI parameters to be explored in diverse renal pathologies, to evaluate whether they are specific markers of LN and other renal diseases. Finally, the sensitivity and specificity of MRI parameters should be assessed by comparison with the gold standard for the diagnosis of LN—renal biopsy within closely matched time point. Ongoing studies in our lab are correlating qMRI measures with renal biopsy performed within 7 days of MRI in LN subjects. Only after both the accuracy and reproducibility the qMRI measurements are established, multi-parametric qMRI can serve as valid biomarkers in clinical trials of LN.

5. Conclusion

This study evaluated the test–retest repeatability of a multi-parametric renal qMRI protocol including DWI, BOLD, ASL and T1rho MRI along with its clinical utility to differentiate between 10 LN

Please cite this article as: Rapacchi S, et al, Towards the identification of multi-parametric quantitative MRI biomarkers in lupus nephritis, Magn Reson Imaging (2015), http://dx.doi.org/10.1016/j.mri.2015.06.019

patients and 10 healthy subjects. The reproducibility of the 4 MRI modalities ranged from moderate to good (ICC = 0.4–0.91, wsCV ≤ 12%) with a few exceptions. T1rho and ASL RBF demonstrated significant differences between the LN and HN groups. The value of the multi-parametric renal quantitative MRI protocol to characterize renal structure and function awaits evaluations in larger clinical populations.

Disclosure of Conflict of Interest

This study was sponsored by Biogen Idec. Six co-authors (P-C.C, C.W., A.V., L.B., N.W., J.T.) are employees of Biogen Idec.

References

[1] Rivera F, López-Gómez JM, Pérez-García R. Clinicopathologic correlations of renal pathology in Spain. Kidney Int 2004;66:898–904.
[2] Alsuwaida A, Husain S, Alghonaim M, AlOudah N, Alwakeel J, Ullah A, et al. Strategy for second kidney biopsy in patients with lupus nephritis. Nephrol Dial Transplant 2011:gfr517.
[3] Guidance for industry on lupus nephritis caused by systemic lupus erythematosus—developing medical products for treatment. http://www.regulations.gov/#!documentDetail;D=FDA-2010-D-0249-0002.
[4] Zhang JL, Morrell G, Rusinek H, Sigmund EE, Chandarana H, Lerman LO, et al. New magnetic resonance imaging methods in nephrology. Kidney Int 2014;85(4):768–78.
[5] Le Bihan D, Breton E, Lallemand D, Aubin ML, Vignaud J, Laval-Jeantet M. Separation of diffusion and perfusion in intravoxel incoherent motion MR imaging. Radiology 1988;168:497–505.
[6] Zhang JL, Morrell G, Rusinek H, Sigmund EE, Chandarana H, Lerman LO, et al. Variability of renal apparent diffusion coefficients: limitations of the monoexponential model for diffusion quantification. Radiology 2010;254:783–92.
[7] Thoeny HC, De Keyzer F, Oyen RH, Peeters RR. Diffusion-weighted MR imaging of kidneys in healthy volunteers and patients with parenchymal diseases: initial experience. Radiology 2005;235:911–7.
[8] Togao O, Doi S, Kuro-o M, Masaki T, Yorioka N, Takahashi M. Assessment of renal fibrosis with diffusion-weighted MR imaging: study with murine model of unilateral ureteral obstruction. Radiology 2010;255:772–80.
[9] Epstein FH, Veves A, Prasad PV. Effect of diabetes on renal medullary oxygenation during water diuresis. Diabetes Care 2002;25:575–8.
[10] Textor SC, Glockner JF, Lerman LO, Misra S, McKusick MA, Riederer SJ, et al. The use of magnetic resonance to evaluate tissue oxygenation in renal artery stenosis. J Am Soc Nephrol 2008;19:780–8.
[11] Thoeny HC, Zumstein D, Simon-Zoula S, Eisenberger U, De Keyzer F, Hofmann L, et al. Functional evaluation of transplanted kidneys with diffusion-weighted and BOLD MR imaging: initial experience. Radiology 2006;241:812–21.
[12] Fenchel M, Martirosian P, Langanke J, Giersch J, Miller S, Stauder NI, et al. Perfusion MR imaging with FAIR True FISP spin labeling in patients with and without renal artery stenosis: initial experience. Radiology 2006;238:1013–21.
[13] Robson PM, Madhuranthakam AJ, Dai W, Pedrosa I, Rofsky NM, Alsop DC. Strategies for reducing respiratory motion artifacts in renal perfusion imaging with arterial spin labeling. Magn Reson Med 2009;61:1374–87.
[14] He X, Moon C, Kim J, Bae KT. In vivo T1ρ study on human kidney. Proc ISMRM 19, 2011, p824.
[15] Wang Y-XJ, Yuan J, Chu ESH, Go MY, Huang H, Ahuja AT, et al. T1ρ MR imaging is sensitive to evaluate liver fibrosis: an experimental study in a rat biliary duct ligation model. Radiology 2011;259:712–9.
[16] Zhang JL, Sigmund EE, Rusinek H, Chandarana H, Storey P, Chen Q, et al. Optimization of *b*-value sampling for diffusion-weighted imaging of the kidney. Magn Reson Med 2012;67:89–97.
[17] He X, Aghayev A, Gumus S, Ty Bae K. Estimation of single-kidney glomerular filtration rate without exogenous contrast agent. Magn Reson Med 2014;71:257–66.
[18] Wu W-C, Fernández-Seara M, Detre JA, Wehrli FW, Wang J. A theoretical and experimental investigation of the tagging efficiency of pseudocontinuous arterial spin labeling. Magn Reson Med 2007;58:1020–7.
[19] McCommis KS, He X, Abendschein DR, Gupte PM, Gropler RJ, Zheng J. Cardiac 17O MRI: Toward direct quantification of myocardial oxygen consumption. Magn Reson Med 2010;63:1442–7.
[20] Wang DJJ, Bi X, Avants BB, Meng T, Zuehlsdorff S, Detre JA. Estimation of perfusion and arterial transit time in myocardium using free-breathing myocardial arterial spin labeling with navigator-echo. Magn Reson Med 2010;64:1289–95.
[21] Avants BB, Epstein CL, Grossman M, Gee JC. Symmetric diffeomorphic image registration with cross-correlation: evaluating automated labeling of elderly and neurodegenerative brain. Med Image Anal 2008;12:26–41.
[22] Klein A, Andersson J, Ardekani BA, Ashburner J, Avants B, Chiang MC, et al. Evaluation of 14 nonlinear deformation algorithms applied to human brain MRI registration. NeuroImage 2009;46:786–802.
[23] Jerome NP, Orton MR, d' Arcy JA, Collins DJ, Koh D-M, Leach MO. Comparison of free-breathing with navigator-controlled acquisition regimes in abdominal diffusion-weighted magnetic resonance images: effect on ADC and IVIM statistics. J Magn Reson Imaging 2014;39:235–40.
[24] Wang J, Zhang Y, Wolf RL, Roc AC, Alsop DC, Detre JA. Amplitude-modulated continuous arterial spin-labeling 3.0-T perfusion MR imaging with a single coil: feasibility study. Radiology 2005;235:218–28.
[25] Altman DG, Bland JM. Measurement in medicine: the analysis of method comparison studies. J R Stat Soc Ser Stat 1983;32:307–17.
[26] Simon-Zoula SC, Hofmann L, Giger A, Vogt B, Vock P, Frey FJ, et al. Non-invasive monitoring of renal oxygenation using BOLD-MRI: a reproducibility study. NMR Biomed 2006;19:84–9.
[27] Li L-P, Storey P, Pierchala L, Li W, Polzin J, Prasad P. Evaluation of the reproducibility of intrarenal R2* and ΔR2* measurements following administration of furosemide and during waterload. J Magn Reson Imaging 2004;19:610–6.
[28] Cutajar M, Thomas DL, Hales PW, Banks T, Clark CA, Gordon I. Comparison of ASL and DCE MRI for the non-invasive measurement of renal blood flow: quantification and reproducibility. Eur Radiol 2014:1–9.
[29] Zhang JL, Rusinek H, Chandarana H, Lee VS. Functional MRI of the kidneys. J Magn Reson Imaging 2013;37:282–93.
[30] Pedrosa I, Alsop DC, Rofsky NM. Magnetic resonance imaging as a biomarker in renal cell carcinoma. Cancer 2009;115(10 Suppl.):2334–45.
[31] Namimoto T, Yamashita Y, Mitsuzaki K, Nakayama Y, Tang Y, Takahashi M. Measurement of the apparent diffusion coefficient in diffuse renal disease by diffusion-weighted echo-planar MR imaging. J Magn Reson Imaging 1999;9:832–7.
[32] Toyoshima S, Noguchi K, Seto H, Shimizu M, Watanabe N. Functional evaluation of hydronephrosis by diffusion-weighted MR imaging. Relationship between apparent diffusion coefficient and split glomerular filtration rate. Acta Radiol 2000;41:642–6.
[33] Michaely HJ, Metzger L, Haneder S, Hansmann J, Schoenberg SO, Attenberger UI. Renal BOLD-MRI does not reflect renal function in chronic kidney disease. Kidney Int 2012;81:684–9.
[34] Akita H, Jinzaki M, Akita A, Mikami S, Oya M, Kuribayashi S. Renal cell carcinoma in patients with acquired cystic disease of the kidney: assessment using a combination of T2-weighted, diffusion-weighted, and chemical-shift MRI without the use of contrast material. J Magn Reson Imaging 2014;39(4):924–30.
[35] Hammer S, de Vries APJ, de Heer P, Bizino MB, Wolterbeek R, Rabelink TJ, et al. Metabolic imaging of human kidney triglyceride content: reproducibility of proton magnetic resonance spectroscopy. PLoS One 2013;8:e62209.

Please cite this article as: Rapacchi S, et al, Towards the identification of multi-parametric quantitative MRI biomarkers in lupus nephritis, Magn Reson Imaging (2015), http://dx.doi.org/10.1016/j.mri.2015.06.019